# UNIVERSITY GRANTS COMMISSION BAHADUR SHAH ZAFAR MARG NEW DELHI – 110 002

Proforma for submission of information at the time of sending the final report of the work done on the project

1. Title of the Project : Identification, purification and characterization of protein

phosphatases PP1 from Leishamania donovani

2. Name and Address of the : Dr. Insaf Ahmed Qureshi,

**Principal Investigator** Department of Biotechnology & Bioinformatics,

School of Life Sciences, University of Hyderabad, Prof. C.R. Rao Road, Hyderabad 500046, India

3. Name and Address of the : University of Hyderabad, Prof. C.R. Rao Road,

**Institution** Hyderabad 500046, India

**4. UGC Approval Letter** : 41-561/2012 (SR), dated 18.7.2012

No. and Date

**5. Date of Implementation** : 01.07.2012

**6. Tenure of the Project** : Three years

7. Total Grant Allocated : Rs. 7,87,500

8. Total Grant Received : Rs. 7,42,500

**9. Final Expenditure** : Rs. 7,42,033

## 10. Title of the Project:

Identification, purification and characterization of protein phosphatases PP1 from *Leishamania donovani* 

## 11. Objectives of the Project:

- Identification and cloning of protein phosphatases (PP1) from *Leishmania donovani*.
- Expression and purification of PP1 proteins using chromatographic methods.
- Characterization of purified proteins through biochemical approaches.
- Structural analysis of PP1 proteins using bioinformatic tools.

# 12. Whether Objectives were achieved:

# Objective 1: Identification and molecular cloning of lesihmanial PP1:

The genome of *L. donovani* is not annotated yet, thus gene sequences of protein phosphatase were identified using an algorithm BLASTn. In *L. major*, this PP1 gene shows eight isoforms but only five isoforms were found in *L. donovani*. Gene specific primers were designed for three ORFs (designated as PP1-3, 1-4 and 1-7). For amplification of the ORFs, gradient PCR was performed with different temperatures and MgSO<sub>4</sub> concentrations. Open reading frame (ORF) of PP1-4 was amplified at 48°C annealing temperature and 2.2 mM MgCl<sub>2</sub> concentration, whereas PP1-3 and 1-7 were amplified at 50°C but with different MgCl<sub>2</sub> concentrations (i.e. 2.5 and 2.0mM respectively). The size of amplified products corresponds to ~1kb (Fig. 1a, c & e). All inserts were separately cloned into pTZ57R/T vector and sequenced. Sequencing results have shown that the sequences were intact without any mutation in the ORF. An insert of ~1kb was released upon digestion of cloned vectors with *Nde* I & *Sal* I restriction enzymes and orientation of the insert was tested by gene specific forward primer and T7 reverse primer. Inserts of PP1-3, 1-4 and 1-7 were sub-cloned into expression vector pET28b and confirmed by restriction analysis using *Nde* I & *Sal* I (Fig. 1b, d & f).

# Objective 2: Over-expression & purification of leishmanial PP1:

For expression of PP1-3, 1-4 and 1-7, different concentrations of IPTG were used for different time duration as well as temperature and result was analyzed on SDS-PAGE. Maximum expression of PP1-3 was observed with 0.6mM concentration of IPTG for 6 hours at 37°C (Fig. 2a), while PP1-4 and 1-7 expressed maximum with 0.4mM of IPTG concentration at 37°C for 4 hours. The observed molecular weight of expressed protein for PP1-3, 1-4 and 1-7 on SDS-PAGE were approximately 35, 42 and 45 kDa respectively.

For further analysis, the cultures were subjected to sonication and found that PP1-3 and 1-4 were completely going in to the pellet (insoluble fraction). Hence, this problem was solved by inducing culture with 0.4 mM IPTG for 20 hours at 18°C and sonication of cell pellet in phosphate buffer in combination with 300mM NaCl, 2 mM BME and 0.3 to 1% sarcosyl to get protein in the soluble fraction. About 40% of protein was observed in supernatant and the rest in the pellet. While in the case of PP1-7, approximately 40-50% of protein was in supernatant without using any detergent and remaining was in pellet (insoluble). The soluble fractions of lysates were subjected to purification by affinity chromatography using Ni-NTA agarose beads. In case of PP1-7, desired protein was eluted with 25 mM, concentration of imidazole (Fig. 2c), while PP1-3 and 1-4 was eluted with 400 and 550 mM concentration of imidazole respectively (Fig. 2a-b). In order to establish the oligomeric state in solution, purified PP1-7 was loaded on to pre-equilibrated Superdex 75 10/300 GL column on AKTA-FPLC (GE HealthCare). PP1-7 was eluted at 10.6 ml as one predominant peak, corresponding to the value close to 45 kDa (Fig. 2d) suggesting the monomeric nature of PP1-7.

## Objective 3: Characterization of purified proteins through biochemical approaches:

#### (a) Circular dichroism measurements:

CD spectroscopy was used to understand the structural contents of PP1-4 and PP1-7. The far-UV CD spectrums displayed a negative peak at 222 and 208 nm that indicates significant secondary structure. Consequently, analysis of secondary structure content with DichroWeb online server using K2D programme suggested  $\alpha$ -helical and  $\beta$ -sheet content to be 29% and 17% for PP1-7, whereas 46% and 27% for PP1-4 respectively (Fig. 3a-b). Simultaneously PP1-7 stability was analyzed at varying pH and temperature which displayed no significant changes in secondary structure content from pH 3.5 to 8.5. But secondary structure spectrum was significantly reduced at pH 9.5 with shift in ellipticity from 208 nm to 204 nm which indicates loss of secondary structure content (Fig. 3c). Similar observations were obtained for near-UV spectra, where negative peaks from 265 to 280 nm in the aromatic region indicated adequate tertiary structure from pH 3.5 to 8.5, but almost negligible at higher pH 9.5 (Fig. 3d). The thermal denaturation data was initially normalized and plotted with temperature versus fraction unfolded which had shown sigmoidal curve with cooperative unfolding started at 310 K, while complete unfolding was achieved at 361 K (Fig. 3e). Further to ascertain thermal melting point (T<sub>m</sub>), enthalpy (ΔH) and heat capacity ( $\Delta$ Cp) of PP1-7, the data was fit to Two-state equilibrium unfolding model using Sigma Plot 12.0. The thermodynamic parameters such as Tm, ΔH and ΔCp were determined to be 315.87  $\pm$  0.26 K, 80.27  $\pm$  5.66 kcal mol<sup>-1</sup> and 2.96  $\pm$  2.44 kcal mol<sup>-1</sup> K<sup>-1</sup> respectively.

#### (b) Fluorescence measurements:

Protein sequences of PP1-4 and PP1-7 contain three and four tryptophan residues respectively. Intrinsic fluorescence spectra of PP1-4 and PP1-7 had shown maximum emission at 330 nm and 324 nm respectively (Fig. 4a). In case of PP1-7 there was no significant shift in emission from pH 3.5 to pH 8.5. At pH 9.5, there was about 15 nm red shift in maximum emission from 324 nm to 339 nm that infers change in conformation of protein and exposure of tryptophan residues to solvent environment (Fig. 4b). Fluorescence quenching studies was performed using acrylamide and quenching effect was observed with increasing concentration of acrylamide. The quenching constant was determined to be  $11.1 \pm 0.2 \text{ mM}^{-1}$  using Stern-Volmer plot (Fig. 4c). Simultaneously, attempts were made to perform the quenching studies in presence of potassium iodide but no effect was observed which points towards buried position of tryptophan residues in the hydrophobic regions that are not exposed to solvent environment. The unfolding studies of PP1-7 were performed using urea from 0 to 4 M and there was red shift of 20 nm in the maximum emission from 324 nm to 344 nm. The data was fit in Two-state equation to determine the free energy ( $\Delta$ G), which was found to be  $2.0 \pm 1.1 \text{ kcal mol}^{-1}$  (Fig. 4d).

## (c) Enzymatic assay and kinetic studies:

PP1-7 phosphatase activity was assayed with artificial substrate pNPP in presence of  $MgCl_2$  or  $MnCl_2$  at varying pH and the hydrolysis of pNPP was maximum at pH 8.5. The phosphatase assay confirmed that purified PP1-7 was enzymatically active and its activity was dependent on the divalent ions i.e.  $Mg^{2+}$  or  $Mn^{2+}$ . Kinetic parameter of PP1-7 revealed a  $K_m$  value 3.14  $\pm$  0.07

and  $5.88 \pm 0.36$  mM in the presence of 5 mM MnCl<sub>2</sub> and 5 mM MgCl<sub>2</sub> respectively (Fig. 5a-b). The  $k_{cat}$  value of PP1-7 was found to be  $0.75 \pm 0.01$  and  $0.06 \pm 0.003$  s<sup>-1</sup> in the presence of 5 mM MnCl<sub>2</sub> and 5 mM MgCl<sub>2</sub> respectively, which indicates the product formation is higher in case of manganese ions than magnesium ions per unit time. Specific activity ( $k_{cat}/K_m$ ) of PP1-7 in the presence of Mn<sup>2+</sup> and Mg<sup>2+</sup> was  $238.85 \pm 3.18$  and  $10.34 \pm 0.74$  M<sup>-1</sup>s<sup>-1</sup> respectively.

## (d) Inhibition studies:

The effect of various known phosphatase inhibitors was tested on the enzymatic activity of purified PP1-7 using pNPP as substrate. Among the general phosphatase inhibitors, sodium tartrate did not affect the activity, while sodium phosphatase, sodium pyrophosphate and sodium fluoride showed significant inhibition in dephosphorylation by PP1-7. Furthermore significant inhibitory effect was observed in presence of sanguinarine that is a known potent inhibitor of PP1-7 family of ser/thr phosphatases. Inhibition studies using sanguinarine had shown the inhibitory effect on PP1-7 with increasing inhibitor concentration. Lineweaver-Burk plot infers the mode of inhibition to be non-competitive with respect to substrate pNPP. The inhibitor constant  $K_i$  for PP1-7 was found to be 0.63  $\mu$ M (Fig. 5a-b).

## Objective 4: Structural analysis of PP1 proteins using bioinformatic tools:

### (a) Homology modeling of protein phosphatases:

Sequence comparison of PP1-7 with a non-redundant sequence database using Protein BLAST software displayed similarities with phosphotases of trypanosomatid parasites including *Leptomonas*, *Trypanosoma* etc. Additionally, the sequence alignment presented homology with PP1-7 phosphatases ranging from 40 to 48% (identity from 25 to 31%) using PDB database. Since crystallographic/solution structure of PP1-7 is not available, three-dimensional structure was predicted to provide structural insights into the catalytic mechanism of leishmanial PP1-7. Human (PDB ID: 3FXJ), which showed 31% identity and 48% similarity along with 69% query coverage and 2e-35 e-value was used as a template for homology modeling using Modeller 9.16. Whereas BLASTp analysis revealed there was no template available for first 64 amino acid residues and these residues are also not involved in the active site. Hence, these residues were trimmed and three-dimensional model of PP1-4 was generated using human (PDB ID: 1JK7) that showed 67.5% identity and 48% similarity along with 74% query coverage and 5e-147 e-value.

The generated models were validated through standard tools and model with minimum energy and structural geometry was selected for further analysis. The stereo-chemical quality of modeled structure was assessed using RAMPAGE revealed seventeen and two residues were found in disallowed region for PP1-7 and PP1-4 respectively. Hence, ModLoop server was used for refinement and then only one amino acid residue (Pro142) for PP1-7 and no residue for PP1-4 was found in disallowed region. Furthermore, energy-minimized structure was validated by superimposition of template to calculate RMSD, which was found to be 1.003 Å and 0.25 Å respectively and then used for performing molecular docking to rationalize the protein-ligand interaction. Structural analysis of predicted model revealed that PP1-7 consist of characteristic core structure of proteins belongings to PP1-7 sub-family, constituted by eleven β-sheets (β1 to

 $\beta$ 11) sandwiched between five  $\alpha$ -helices ( $\alpha$ 1 to  $\alpha$ 5) on one side and seven  $\alpha$ -helices ( $\alpha$ 6 to  $\alpha$ 12) on the other side of the sheet (Fig. 7a). While, structure of PP1-4 is composed of ten  $\alpha$ -helices and eleven  $\beta$ -sheets (Fig. 8a).

AutoDock Vina was used for molecular docking studies and docked conformation with the lowest binding energy was taken as highly plausible binding conformation. Among the nine complexes, configuration 3 was considered as the best complex with binding energy of -5.3 kcal mol<sup>-1</sup> for docking of substrate pNPP to PP1-7. Phosphate group of pNPP forms hydrogen bonds with Arg33, Asp55, Gly56, and Asp265 residues, while nitro group interacts with Arg169, Ser173 and Ala175. Simultaneously, docking of sanguinarine with PP1-7 suggested a new site for binding instead of active site, which is formed by residues present in loop region between  $\alpha$ 11 and  $\alpha$ 12. Sanguinarine docked on this site through interaction with Glu336 and Asn346 residues of PP1-7 with docking energy of -8.9 kcal mol<sup>-1</sup> (Fig. 7b).

# (b) Inhibitor and metal binding sites:

Structure superimposition showed that the active site of PP1-7 is located at a cleft between two central beta sheets that contains a binuclear metal ion site essential for catalysis. Metal binding pattern of PP1-7 was quite similar to structures of human PP (PDB ID: 1A6Q and 3FXJ) that also displays two manganese ions in binding site. Amino acid residues Asp55, Asp221 and Asp265 coordinate the first metal ion into M1 site, while Asp55 and Gly56 coordinate the second metal ion into M2 site (Fig. 7c). Another human PP structure (PDB ID: 2IQ1) possess a third metal ion site (M3) in active site in which one Mg<sup>2+</sup> coordinate with Asp127, Gly128 and Asp337 residues. The residues of M3 site (i.e. Asp55, Gly56 and Asp265) was also conserved in PP1-7 structure (Fig. 7d). 3DLigandsite had also predicted the amino acid residues involved in metal binding to be Asp55, Asp221 and Asp265. Simultaneously, superimposition of PP1-4 model structure with human PP (PDB ID: 1JK7) displayed Arg91, Arg217 and Tyr268 coordinates of inhibitor okadaic acid (Fig. 8b).

#### 13. Achievements from the Project:

- 1) Three serine/threonine phosphatases (STPs) were cloned from *L. donovani* into expression vector followed by their purification using chromatographic techniques. Subsequently, molecular mass and enzymatic activity was determined for recombinant PP1-7.
- 2) Purified PP1-4 and 1-7 were characterized using circular-dichroism and fluorescence spectroscopy. Simultaneously, effect of temperature, pH and chemical denaturants were studied to understand the secondary structural changes in PP1-7.
- 3) Three dimensional structure of PP1-4 and 1-7 were predicted using homology modelling followed by study of their interaction with substrate, metal ions as well as specific inhibitor.

#### 14. Summary of the Findings:

In present study, full length ORFs of three protein phosphatases (namely PP1-3, 1-4 and 1-7) were cloned from *L. donovani* into expression vector followed by purification using Ni-NTA

affinity chromatography. Recombinant PP1-7 was found to be enzymatically active and dephosphorylated the substrate pNPP only in presence of manganese or magnesium ions, whereas the activity was inhibited by sanguinarine with a non-competitive mode of inhibition. Gel filtration chromatography suggested that purified PP1-7 is present as a monomer in solution, whereas secondary structure analysis of PP1-4 and 1-7 revealed presence of an appropriate secondary and tertiary structure. CD and fluorescence spectroscopy results indicated towards an adequate protein conformation from pH 3.5 to 8.5. The quenching constant (Ksv) and free energy ( $\Delta G$ ) of PP1-7 was found to be 11.1  $\pm$  0.2mM<sup>-1</sup> and 2.0  $\pm$  1.1 kcal mol<sup>-1</sup> in presence of acrylamide and urea respectively. Computational modelling of PP1-4 and 1-7 showed similar three-dimensional structure and metal binding sites present in other member of ser/thr family of protein phosphatases, while docking studies revealed its interaction with substrate as well as its specific inhibitor. Altogether, our study has provided first time reports on enzyme kinetics and structural features of metal-dependent protein phosphatases from a trypanosomatid parasite.

### 15. Contribution to the Society:

Visceral leishmaniasis, also known as kala-azar, is caused by *L. donovani* and is usually fatal without treatment. Due to unavailability of effective vaccines, the current control measures highly depend on chemotherapy that presents several limitations to eradication of the disease including high cost, toxicity and the emergence of drug resistant strains. Therefore, it is of utmost importance to search for novel chemotherapeutic options for the treatment of leishmaniasis. Out of 58 leishmanial STPs, only 6 phosphatases have been partially studied in spite of their proposed critical role in life cycle of leishmanial parasite. We have cloned and purified three STPs from *L. donovani* followed by characterization of PP1-7 employing various biochemical and structural methods. Our results could be helpful in further studies involving the crystallographic approach with and without ligands which might improve our understanding for catalytic mechanism of phosphatases in leishmanial parasite. Concurrently, further investigation to delineate the importance of PP2C enzymes in leishmanial infection could provide a significant insight into its indispensable myriad of biological functions.

## 16. Whether any Ph.D. Enrolled/Produced Out of the Project:

Not applicable

## 17. No. of Publications out of the Project:

1) Jakkula P, Qureshi R, Iqbal A, Sagurthi SR, Qureshi IA (2018). *Leishmania donovani* PP2C: Kinetics, structural attributes and *in vitro* immune response. *Molecular and Biochemical Parasitology* 223:37-49.

(Principal Investigator)

(Registrar)

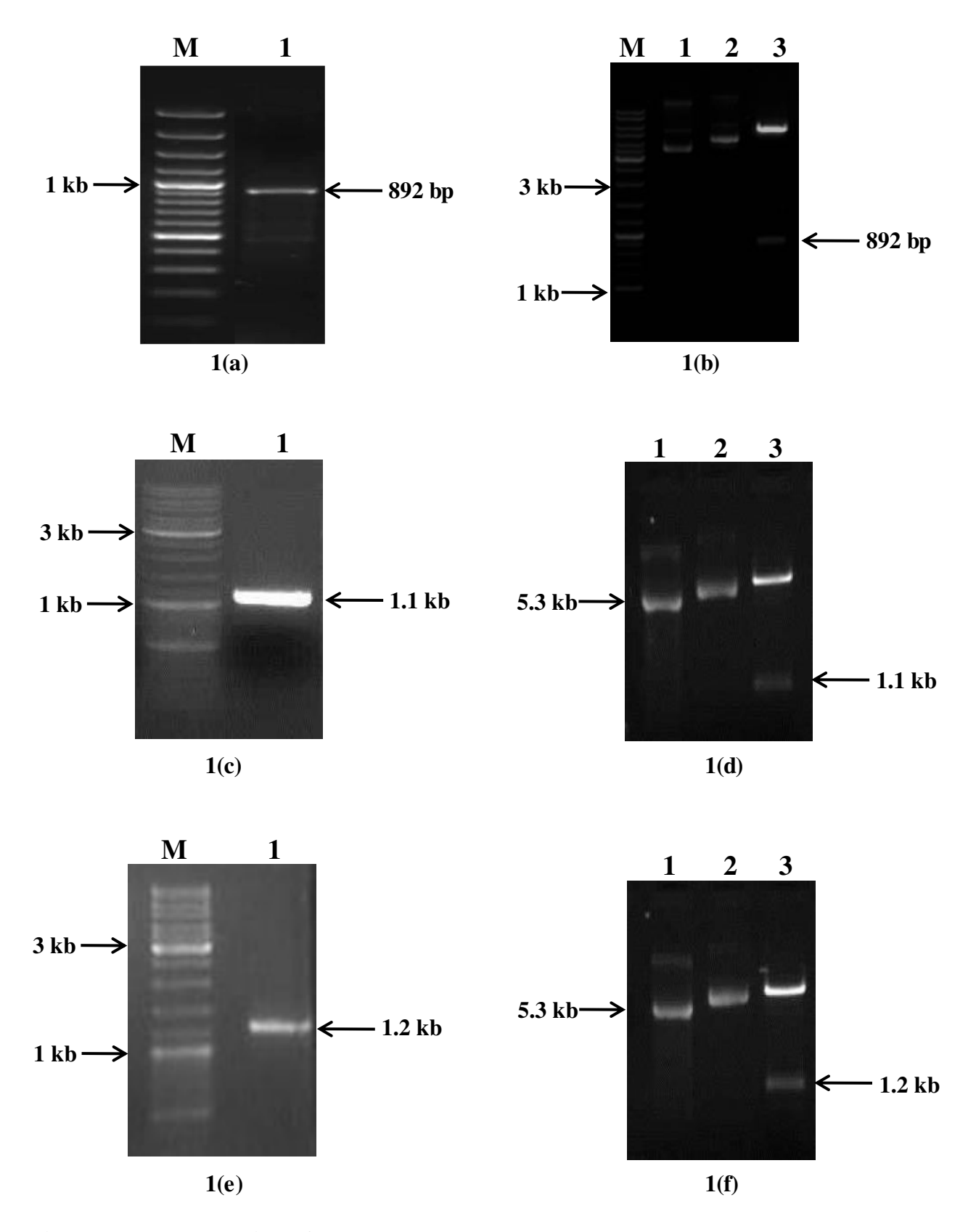


**Fig. 1: Molecular cloning of PP1 Phosphatases.** (a), (c) and (e) PCR amplification of PP1-3, PP1-4 and PP1-7. (b), (d) and (f) Restriction digestion of pET28a:PP1-3, pET28a:PP1-4 and pET28a:PP1-7 with *Nde*I and *Sal*I.

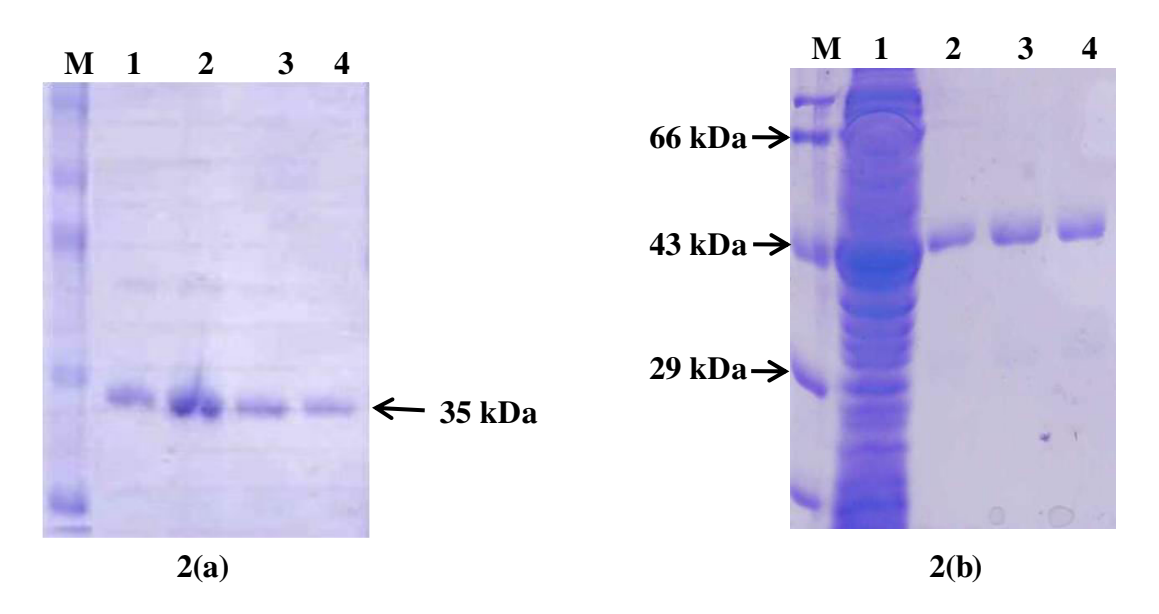


**Fig. 2: Ni-NTA Purification of PP1 phosphatases.** (a) PP1-3 purification gel, Lane 1: protein marker, Lane 2, 3, 4 and 5: purified fractions. (b) PP1-4 purification gel, Lane 1: protein marker, Lane 2: Supernatant, Lane 3, 4 and 5 purified fractions.

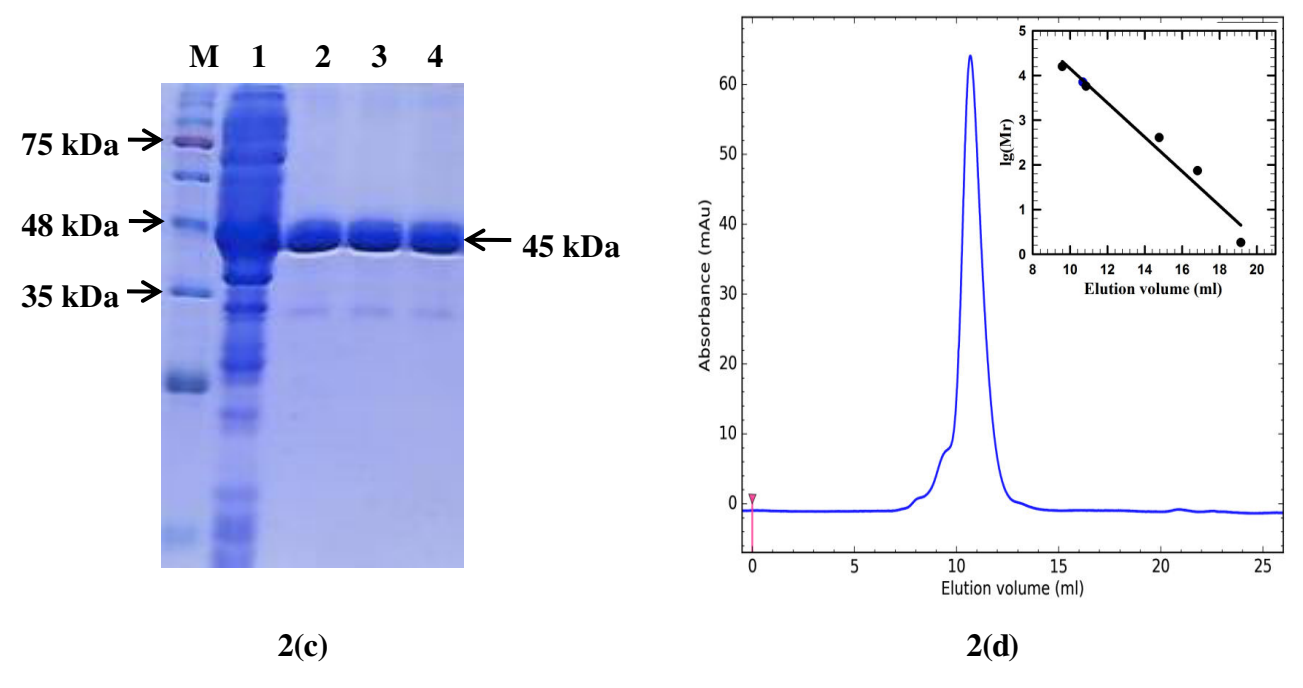


**Fig. 2: Ni-NTA Purification and molecular weight determination of PP1-7**. (c) 12% SDS PAGE; Lane 1: protein marker, Lane 2: supernatant and Lane 3, 4 and 5: purified fractions. (d) Molecular weight determination of PP1-7: Size exclusion chromatography profile of PP1-7 showing elution at 10.6 ml on a Superdex 75 10/300 corresponding to 45 kDa molecular weight.

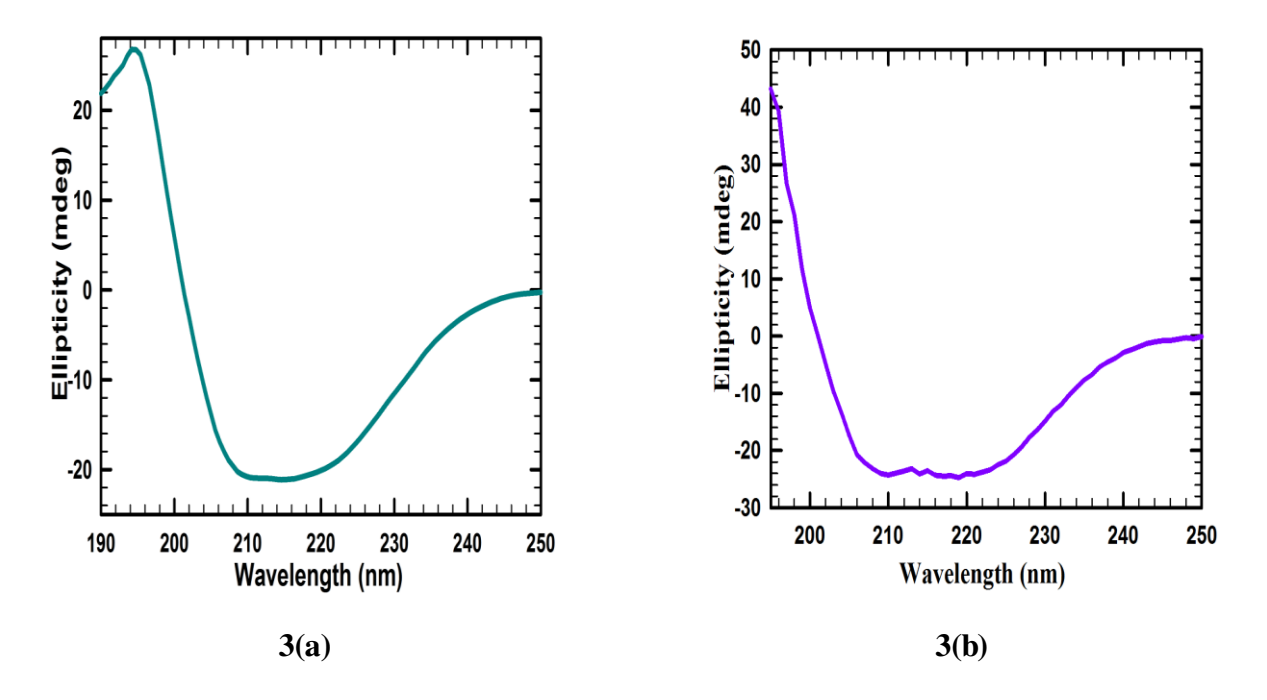
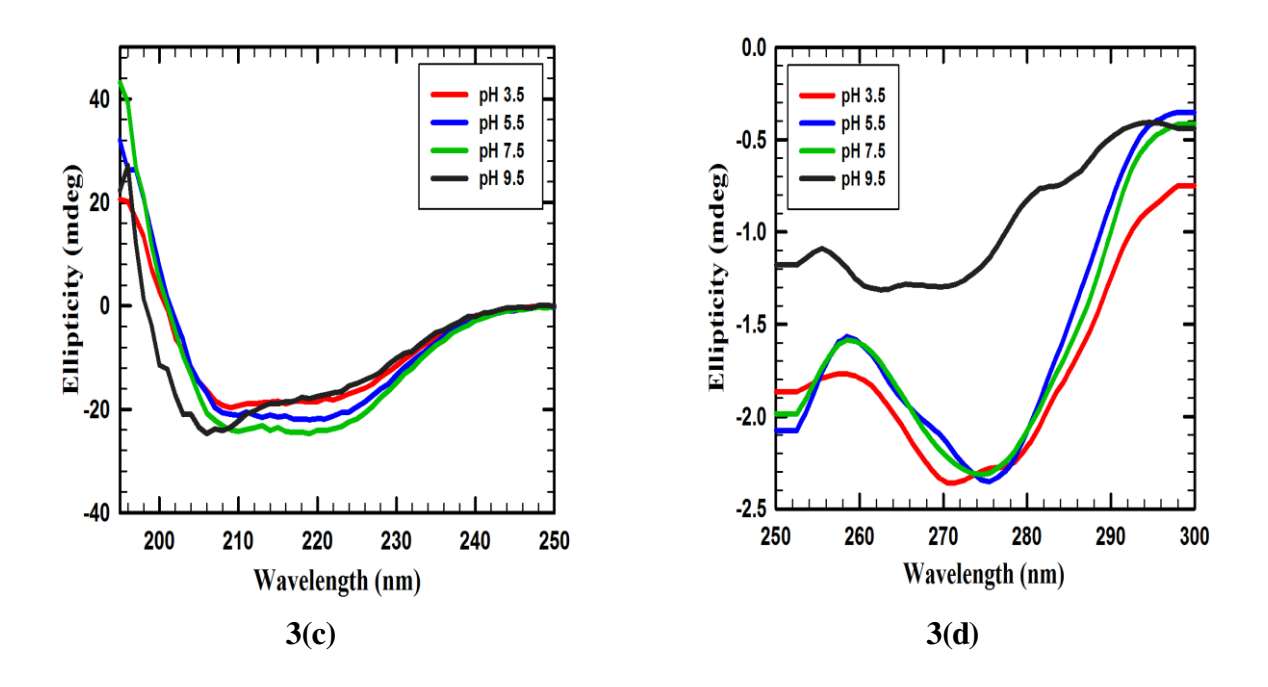
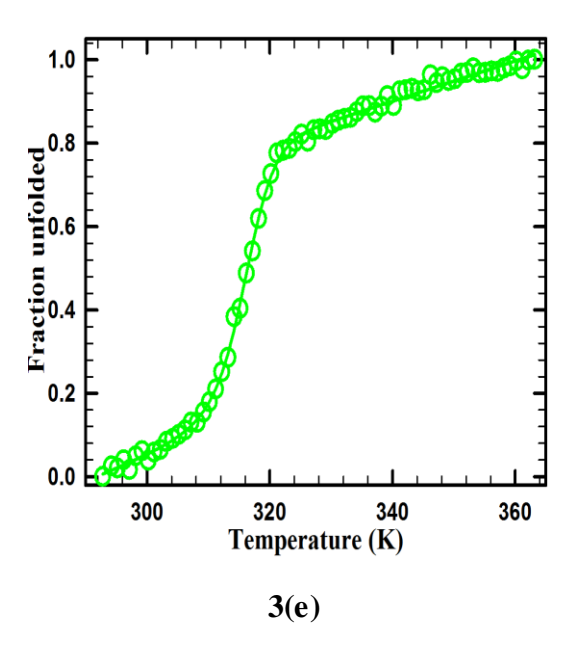


Fig. 3: CD-spectra measurements. (a) Far UV-CD spectra of PP1-4 from 250 to 190 nm using 4.0  $\mu$ M of protein. (b) Far UV-CD spectra of PP1-7 from 250 to 195 nm using 2.5  $\mu$ M of protein.



**Fig. 3:** (c) Far UV-CD and (d) Near UV-CD spectra of PP1-7 at different pH conditions, where pH 3.5, 5.5, 7.5 and 9.5 are presented as red, blue, green, and black line respectively.



**Fig. 3:** (e) Thermal denaturation curve of PP1-7. Thermodynamic parameters were calculated from the Two-state fit of denaturation as a function of temperature.

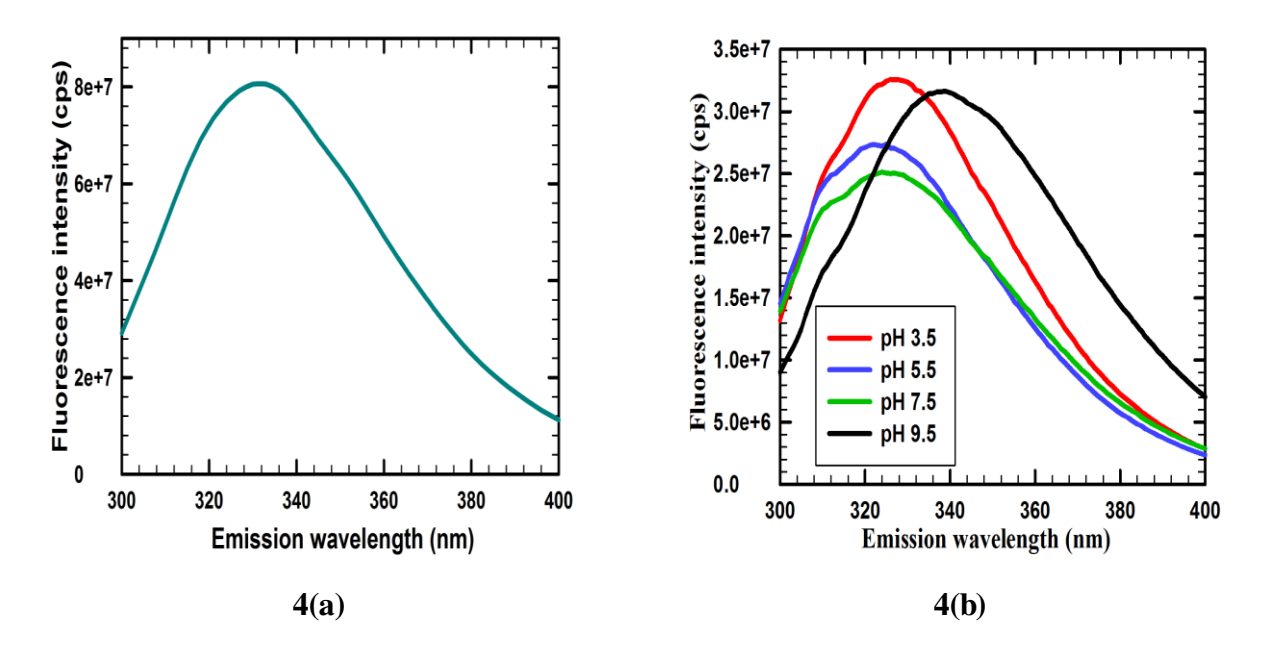


**Fig. 4: Fluorescence measurements.** (a) Intrinsic fluorescence profile of PP1-4 shows emission maxima at 330 nm using 2  $\mu$ M protein. (b) Intrinsic fluorescence profile of PP1-7 at varying pH conditions, where pH 3.5, 5.5, 7.5 and 9.5 are displayed as red, blue, green and black respectively.

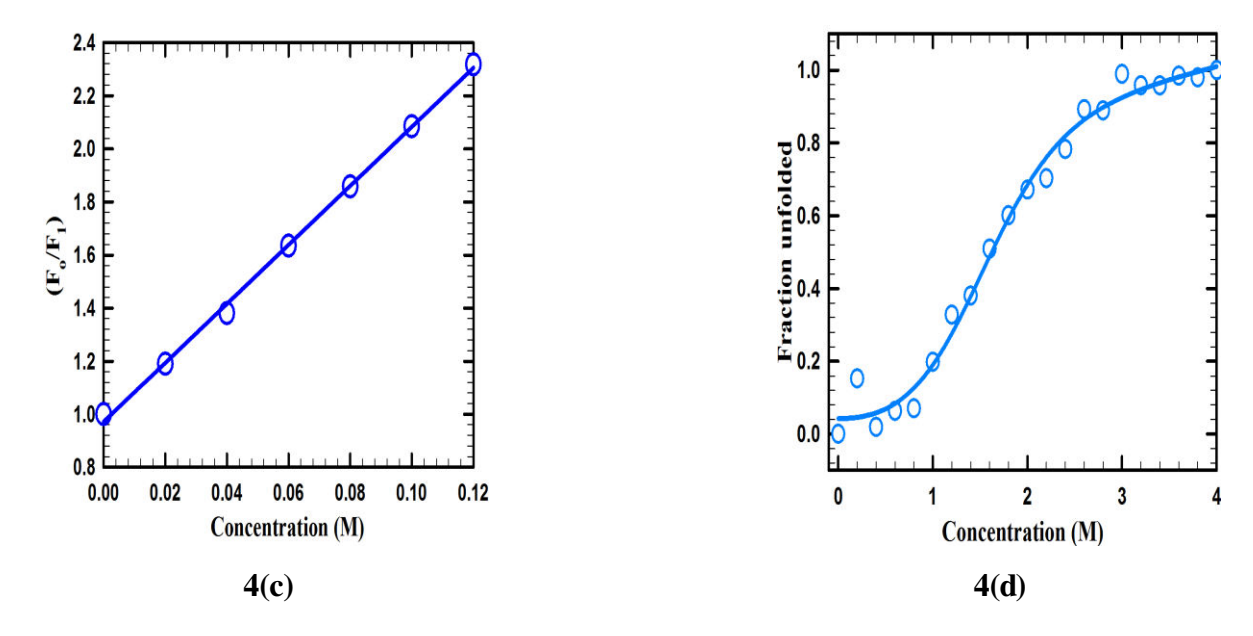


**Fig. 4: Fluorescence measurements of PP1-7.** (c) Analysis of PP1-7 tryptophan fluorescence quenching using Stern-Volmer plot. (d) Normalized urea denaturation curve. Gibbs free energy was calculated by non-linear regression analysis.

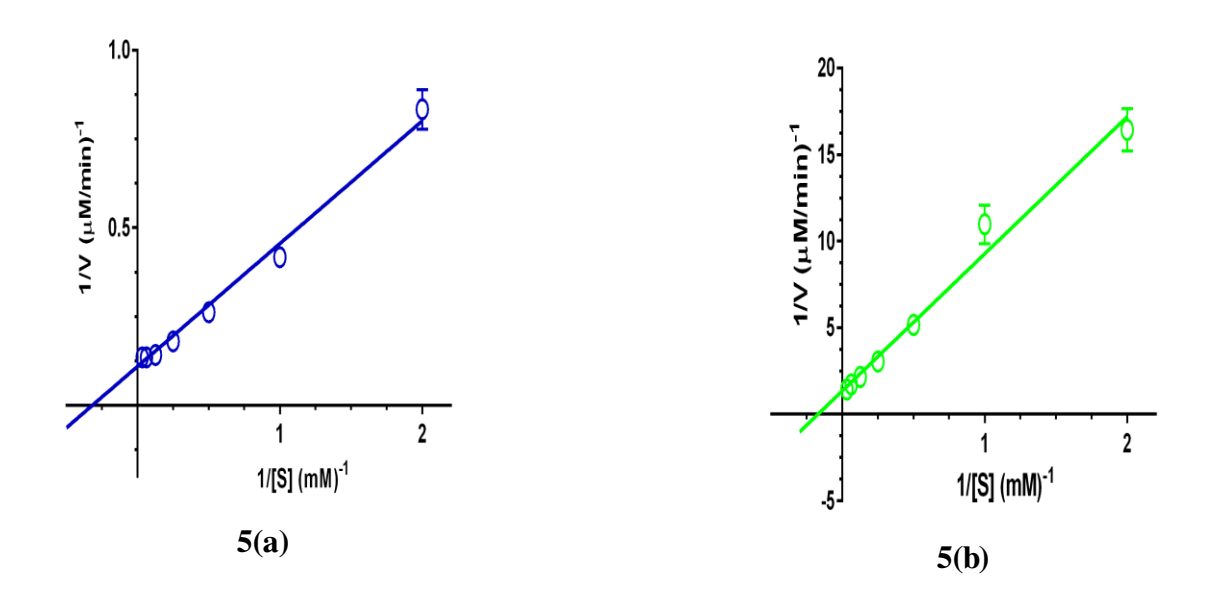
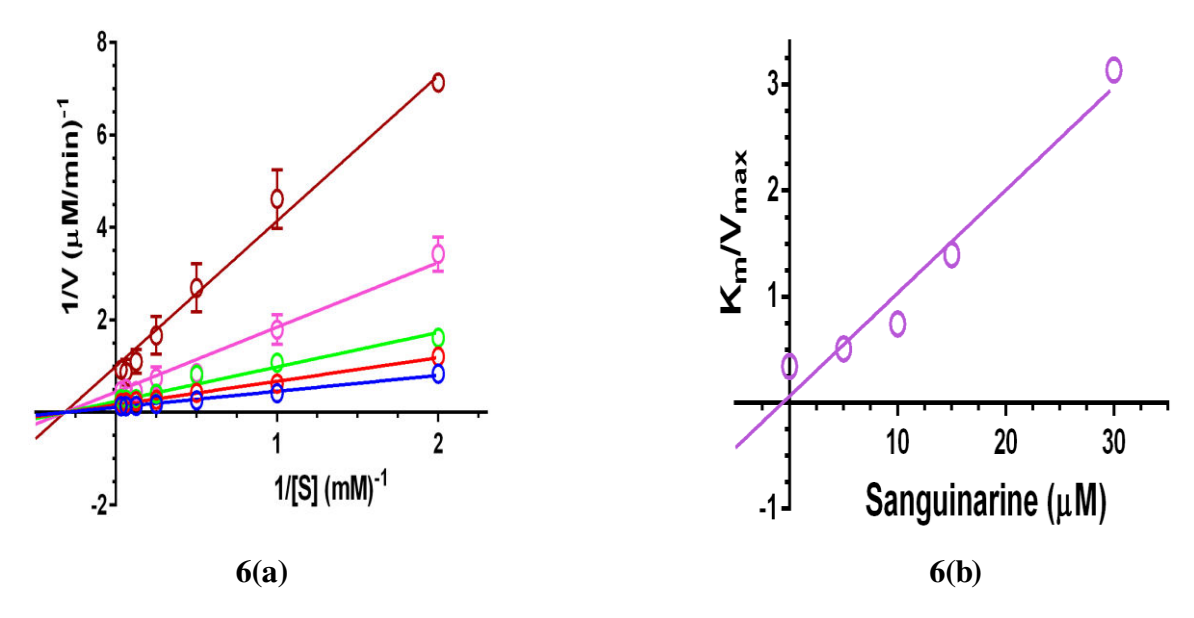


Fig. 5: Enzyme kinetic analysis of PP1-7. The activity was performed with  $0.2 \mu M$  PP1-7 and different concentrations of pNPP in presence of 5mM MnCl<sub>2</sub> (a) and 5mM MgCl<sub>2</sub> (b), and indicated as blue and green circles respectively.



**Fig. 6: Inhibition studies of PP1-7.** (a) Lineweaver-Burk plot for inhibition of PP1-7 using different concentrations of sanguinarine. Blue circles indicate PP1-7 activity without inhibitor, whereas red, green, pink and brown circles depict 5, 10, 15 and 30  $\mu$ M of sanguinarine respectively. (b) Determination of the inhibition parameter ( $K_i$ ) using second plot with the slopes from Lineweaver-Burk plots towards the concentrations of sanguinarine.

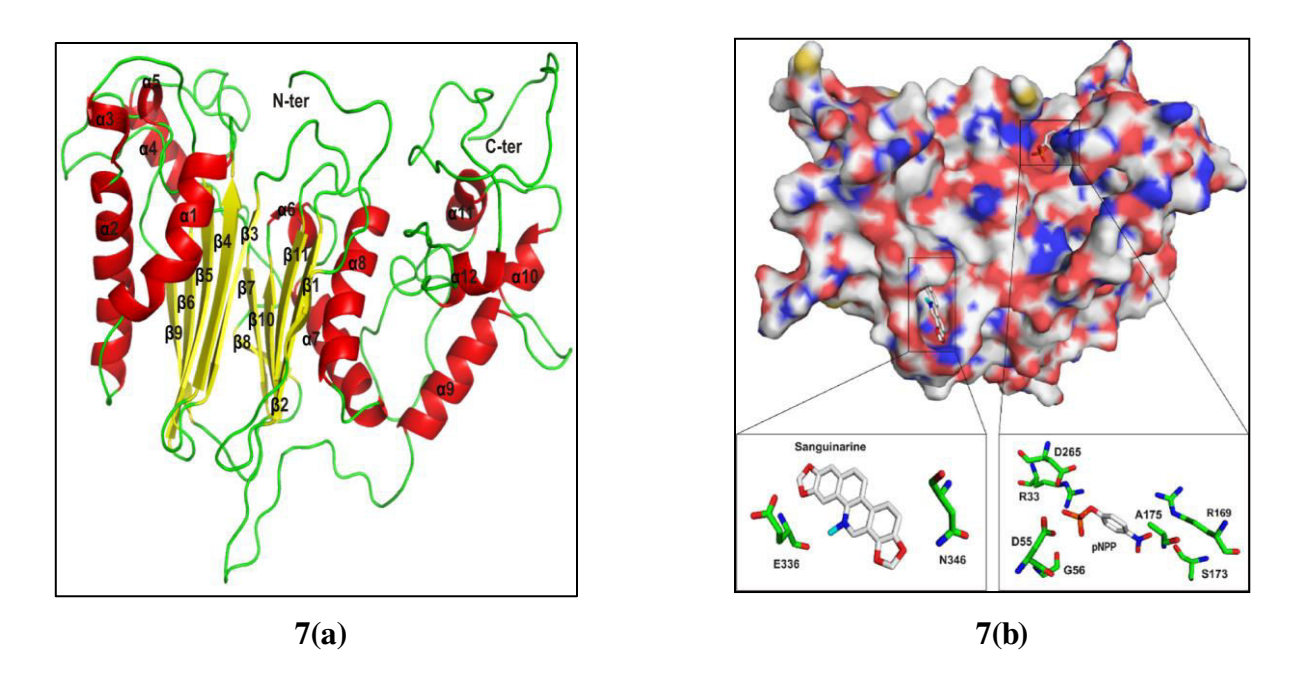
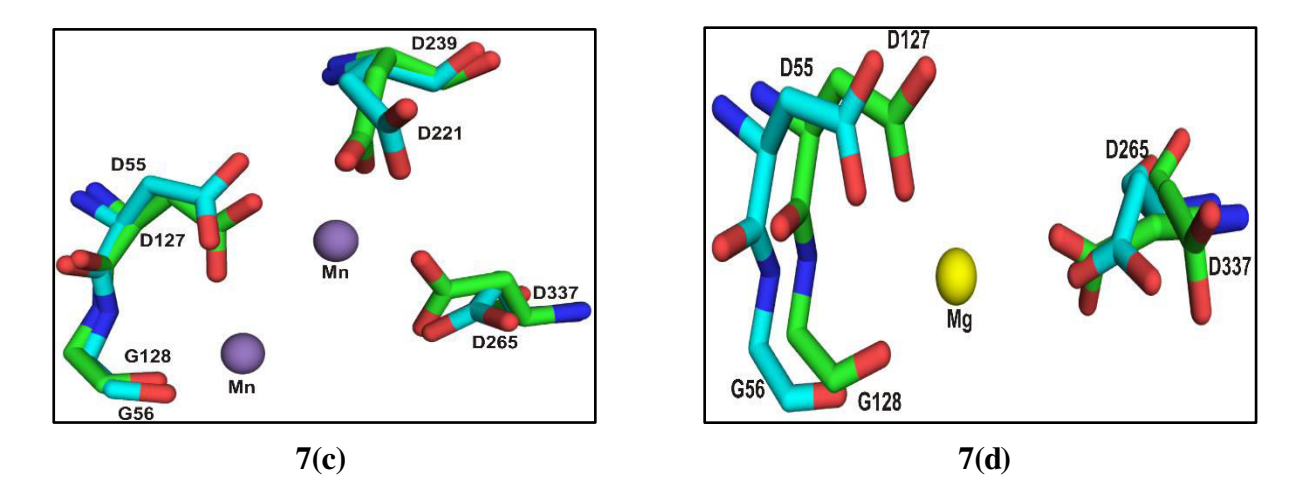
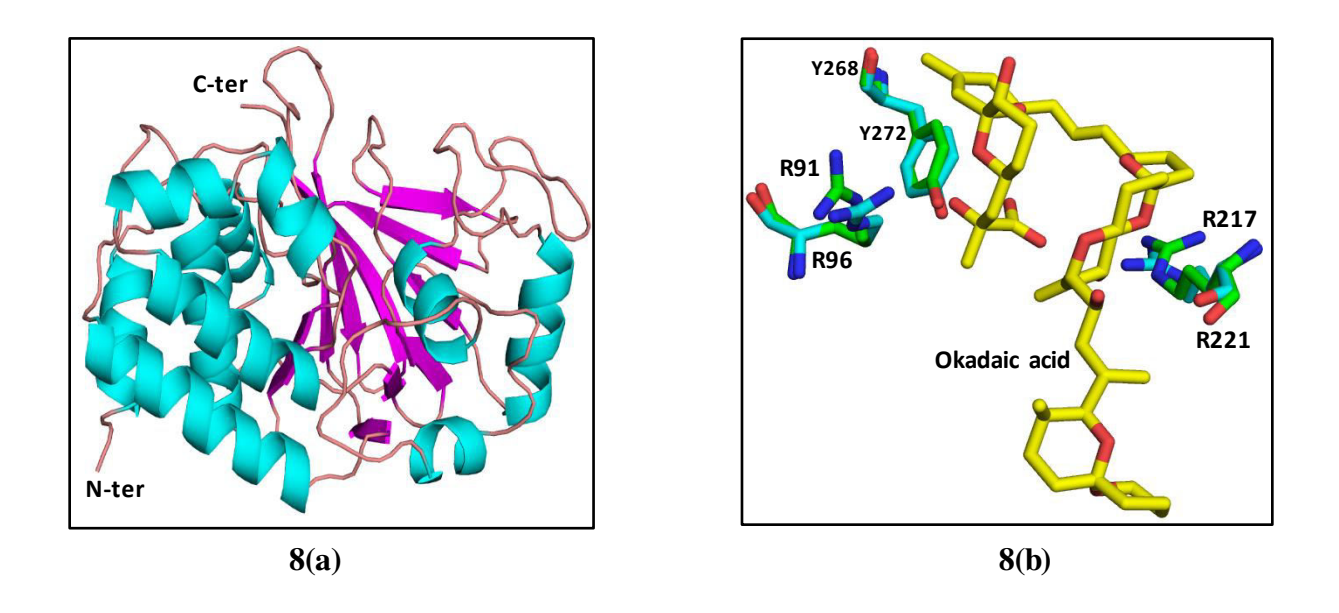


Fig. 7: Modelled 3D-structure and docking studies of PP1-7. (a) Three dimensional structure of PP1-7 model is presented in cartoon view, while  $\alpha$ - helices,  $\beta$ -strands and random coils are represented in red, yellow and green respectively. (b) Docking study of PP1-7 was performed with ligands (sanguinarine and pNPP) using Autodock Vina, while PP1-7 and ligands were presented as electrostatic surface and stick view respectively. The residues showing interaction between protein and ligands are labelled and displayed as stick model in element colors (carbon, nitrogen, oxygen and phosphorus colored green/white, blue, red and orange respectively).



**Fig. 7: Metal binding sites of PP1-7.** Crystal structure of human PP [PDB ID: 2IQ1 (c) and 3FXJ (d)] was superimposed on PP1-7 structure, residues coordinating metals are labelled and represented as cyan (human) and green (PP1-7) sticks. Mn<sup>2+</sup> and Mg<sup>2+</sup> ions are represented as violet and yellow spheres respectively.



**Fig. 8:** Modelled 3D-structure and docking study of PP1-4. (a) Three dimensional structure of PP1-4 model is presented in cartoon view, while  $\alpha$ - helices,  $\beta$ -strands and random coils are represented in cyan, magenta and wheat colors respectively. (b) Docking study of PP1-4 was performed with okadaic acid using Autodock Vina and the residues showing interaction between protein and ligands are labelled and displayed as stick model in element colors (carbon, nitrogen, oxygen and phosphorus colored green/white, blue, red and orange respectively).